Low-Temperature Femtosecond-Resolution Transient Absorption Spectroscopy of Large-Scale Symmetry Mutants of Bacterial Reaction Centers†

Su Lin, Weizhong Xiao,‡ J. Elizabeth Eastman, Aileen K. W. Taguchi, and Neal W. Woodbury*

Department of Chemistry and Biochemistry and the Center for the Study of Early Events in Photosynthesis, Arizona State University, Tempe, Arizona 85287-1604

Received September 13, 1995; Revised Manuscript Received January 3, 1996⊗

ABSTRACT: Reaction centers isolated from three large-scale symmetry mutants, *sym0, sym2−1,* and *sym5−2* described in the previous article of this issue [Taguchi, A. K. W., Eastman, J. E., Gallo, D. M., Jr., Sheagley, E., Xiao, W., & Woodbury, N. W. (1996) *Biochemistry 35,* 3175−3186] have been investigated by low-temperature ground state and femtosecond-resolution transient absorption spectroscopy. All three of these large-scale symmetry mutants undergo electron transfer at 20 K. The mutants *sym0* and *sym5−2* have yields and dominant rates of charge separation comparable to wild type. However, the *sym2−1* mutant shows a roughly 35% quantum yield at this temperature, and the major kinetic component of the initial electron transfer is slower than wild type by nearly a factor of 100. The *sym0* mutant showed substantial changes in the monomer bacteriochlorophyll ground state and transient spectra, and both *sym0* and *sym2−1* showed changes in the bacteriopheophytin ground state and transient spectra. In particular, *sym2−1* shows a small absorbance decrease in the region of the Q_X band of the B side bacteriopheophytin which could be attributed to 10%−20% electron transfer along the B pathway.

Despite the structural symmetry of the bacterial reaction center (Deisenhofer et al., 1984; Allen et al., 1987; Chang et al., 1991; Ermler et al., 1994), previous measurements have indicated that the branching ratio between electron transfer along the A and B sides strongly favors charge separation involving A side cofactors [for reviews of reaction center spectroscopy and function see Kirmaier and Holten (1987, 1993), Feher et al. (1989), Parson (1991), Woodbury and Allen (1995)]. A number of steady state and nanosecond resolution absorbance measurements have been performed in which reaction centers with both the primary quinone (Q_A)[1] and the A side bacteriopheophytin (H_A) reduced have been shown to form the anion of the B side bacteriopheophytin (H_B) with a limited quantum yield (approximately 8%−9%; Tiede et al., 1987; Kellogg et al., 1989). Comparing this yield to the overall decay rate of the initial electron donor excited singlet state (P*) under the same conditions (20 ps with reduced Q_A and H_A; Holten et al., 1978) a branching ratio of 200:1 in favor of the A side was determined (Kellogg et al., 1989). Calculations of relative electron transfer rates along the two paths based on the crystal structure of *Rhodopseudomonas (Rp.) viridis* (Michel-Beyerle et al., 1988) implied a much smaller asymmetry in electron transfer along the two branches (a branching ratio of about 12).

Direct measurements of the absorbance changes associated with P^+H^- formation have also been performed on the picosecond time scale in reaction centers where H_A is not reduced initially. Such measurements should more accurately represent the state of the reaction center found *in vivo* on the time scale of electron transfer than the optical pumping methods. None of these measurements on wild type reaction centers has indicated that picosecond charge separation results in any detectable $P^+H_B^-$ (Kaufmann et al., 1976; Kirmaier et al., 1985; Breton et al., 1986; Bylina et al., 1988; Lockhart et al., 1990). The highest resolution fast transient absorption measurements of the state P^+H^- have been performed at low temperature in *Rb. sphaeroides* R-26 reaction centers (a carotenoidless strain) (Kirmaier et al., 1985; Lockhart et al., 1990). Unfortunately these measurements are not as sensitive to small amounts of electron transfer to H_B as are the photopumping experiments, and it was only possible to set an upper limit of about 10% to the transient population of $P^+H_B^-$.

Similar measurements have also been performed on mutant reaction centers in which the A side bacteriopheophytin was replaced with bacteriochlorophyll (called β). In this mutant, the only major transition in the 530 nm region is the Q_X band of H_B. This makes the spectroscopic detection of B side electron transfer more sensitive by obviating any absorbance changes in the Q_X bacteriopheophytin band due to H_B reduction, even at room temperature (Kirmaier et al., 1991). In this mutant, evidence has been presented for a roughly 3% yield of $P^+H_B^-$ (Heller et al., 1995). The amount of B side electron transfer is apparently increased to about 15% by combining the β-mutation with a second mutation designed to alter the environment of the A side monomer bacteriochlorophyll (B_A), possibly via hydrogen bonding (Heller et al., 1995; Williams et al., 1992). Heller et al.

† This work was supported by grants DMB 91-585251 and MCB 9219378 from the National Science Foundation. Instrumentation was purchased with funds from NSF Grant DIR-8804992 and Department of Energy Grants DE-FG-05-88-ER75443 and DE-FG-05-87-ER75361. This is Publication No. 260 from the Arizona State University Center for the Study of Early Events in Photosynthesis.

* To whom correspondence should be addressed.

‡ Present address: Department of Pathology and Laboratory Medicine, Hospital of University of Pennsylvania, 7−114 Founders, 3400 Spruce St., Philadelphia, PA 19104.

⊗ Abstract published in *Advance ACS Abstracts,* February 15, 1996.

[1] Abbreviations: *Rb., Rhodobacter*; *Rp., Rhodopseudomonas*; P, bacteriochlorophyll dimer; B, monomer bacteriochlorophyll; H, monomer bacteriopheophytin; Q, quinone; wt, wild type; fs, femtosecond; ps, picosecond.

0006-2960/96/0435-3187$12.00/0

(1995) have suggested that the energy of $P^+B_A^-$ is a critical factor in determining the ratio of A side to B side electron transfer.

The work of Heller et al. (1995) supports the concept that the protein environment differentially mediates the free energy of charge-separated states on the two potential electron transfer pathways, an idea that has been suggested previously by others [e.g., Parson et al. (1990), Gehlen et al. (1994), Steffen et al. (1994)]. However, the specific molecular interactions that give rise to this differential control in wild type reaction centers is still unknown. Obviously, the differences between the A and B side electron transfer pathways of the reaction center ultimately stem from differences in the identity of the amino acids which make up their environment. In an attempt to identify the amino acids important in the asymmetry of initial electron transfer, a series of large-scale symmetry mutants, described in the preceding article (Taguchi et al., 1996), were constructed which between them replace 80% of the M subunit amino acids which come in close contact with P, the monomer bacteriochlorophylls, or the bacteriopheophytins with their L subunit counterparts. This report describes femtosecond transient absorbance measurements of electron transfer in three of these mutants.

EXPERIMENTAL PROCEDURES

Mutant Construction and Sample Preparation. The mutants and *Rhodobacter capsulatus* strains used as the source of *sym0*, *sym2−1*, *sym5−2*, and wild type reaction centers in this work as well as the reaction center preparations were described in the preceding article of this issue (Taguchi et al., 1996). Reaction centers prepared in this way contain all of the normal reaction center cofactors except for Q_B which is lost. The stochiometry of the bacteriochlorophylls, bacteriopheophytins, and carotenoid has been determined in the wild type reaction centers by HPLC analysis of extracts (Gallo, 1994). The loss of Q_B from these preparations has been reported previously (Taguchi et al., 1992). The *sym0* reaction centers used here were isolated from the *sys0−4* background strain (Taguchi et al., 1996). The *sym2−1*, *sym5−2*, and wild type reaction centers were isolated from an U43 background (Youvan et al., 1985).

Low-Temperature Ground State and Transient Absorbance Spectroscopy. Low-temperature ground state spectra were recorded as described by Williams et al. (1992). Reaction centers were isolated in LDAO-containing buffer, and rechromatographed into a Triton X-100-containing buffer [Triton buffer: 10 mM KPO_4 buffer (pH 7.35), 0.04% Triton X-100, 150 mM KCl] by binding to a DEAE-Sephacel column (Pharmacia), washing extensively with Triton buffer, and eluting in Triton buffer with high salt. Samples were then dialyzed against Triton buffer, mixed with two parts (v/v) glycerol, and degassed before cooling in a helium displex refrigerator (APD) to 20 K.

Low-temperature femtosecond spectroscopy was performed on samples prepared in the way described above except that 5 mM dithionite was added to reduce the quinones. The femtosecond absorbance apparatus described previously was used (Woodbury et al., 1994; Peloquin et al., 1995). For this work, excitation was at 860 nm using 10 nm wide (full-width at half-maximum), 150 fs duration pulses at a repetition rate of 540 Hz. The pulse intensity was 3−5 μJ over a roughly 2 mm^2 area, and resulted in excitation of 10%−15% of the reaction centers in the sample. For all measurements, a weak probe pulse was produced by continuum generation and spectra were detected with a dual diode array spectrophotometer over a 140 nm spectral range. For long-time kinetic traces (greater than a few hundred picoseconds), a no-excitation base line was recorded and subtracted from the data to remove the small (less than 0.02) absorbance change offset that can occur on that time scale due to small movements in the probe beam positions.

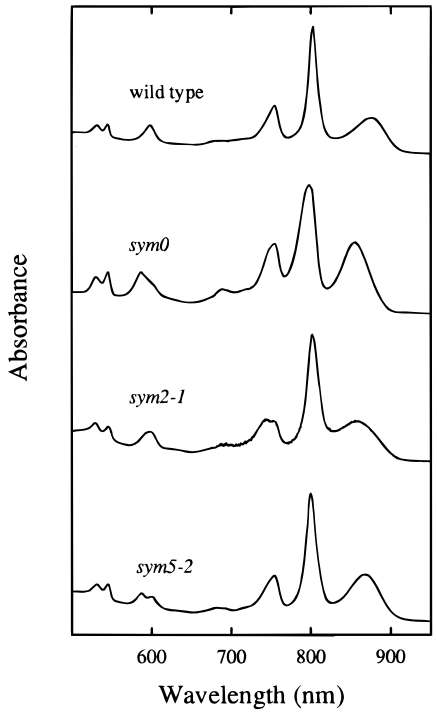

FIGURE 1: Ground state absorbance spectra of wild type, *sym0*, *sym2−1*, and *sym5−2* reaction centers from *Rb. capsulatus* taken in a glycerol glass at 20 K between 500 and 950 nm. Spectra were taken on a Cary 5 spectrophotometer with a spectral resolution of 0.5 nm.

RESULTS

Low-Temperature Ground State Spectra. Figure 1 shows the ground state spectra at 20 K for wild type *Rb. capsulatus* reaction centers and for *sym0*, *sym2−1*, and *sym5−2* reaction centers. The prominent transitions in the near-infrared region of the spectrum from the wild type include the Q_Y band of P at 875 nm, a relatively sharp absorbance peak at 802 nm which includes the Q_Y transitions of the monomer bacteriochlorophylls, and an asymmetric band centered at 755 nm which includes Q_Y transitions from both of the bacteriopheophytins. In the visible region, the Q_X bands of the bacteriopheophytins are resolved at this temperature. The band due to H_A appears at 545 nm, and that due to H_B is seen at 532 nm. The band peaking at 598 nm includes Q_X transitions from all of the bacteriochlorophylls, and in the wild type these transitions are not resolved.

The most dramatic spectral changes are seen in the *sym0* mutant (Figure 1). The Q_Y band of P shifts to shorter wavelength, peaking at 855 nm. The 800 nm band is much broader than that of wild type as well as blue shifted several nanometers (Table 1), and the Q_Y band of the bacteriopheophytins has become distinctly asymmetric. The ratio of the peak intensities of the infrared bands has also changed. The

Table 1: Absorption Band Positions of Reaction Centers Isolated from Wild Type *Rb. capsulatus* and Its Mutants

reaction center	P	B	H (Q_Y) H_A/H_B	B (Q_X)	H (Q_X) H_A/H_B
wild type	875	802	755	598	545/532
sym0	855	798	755	587	545/531
sym2−1	855	802	754/743	599	546/529
sym5−2	868	800	754	587/600	545/532

peak of the broad transition near 800 nm is substantially lower in intensity relative to the Q_Y transition of P and the Q_X transitions in the 540 and 600 nm regions. In the visible region, additional resolution of the bacteriochlorophyll transitions between 590 and 600 nm is also observed.

In reaction centers isolated from *sym2−1*, the Q_Y band of P is again shifted to 855 nm and the bacteriopheophytin Q_Y transitions are resolved at 743 and 754 nm. As with *sym0*, additional resolution of the bacteriochlorophyll Q_X transitions is observed in this mutant.

The spectral features of reaction centers isolated from *sym5−2* are generally very similar to wild type reaction centers except that the bacteriochlorophyll Q_X transitions are particularly well resolved into two peaks at 587 and 600 nm. A detailed comparison of the peak wavelengths of the resolved transitions in each of the spectra in Figure 1 is given in Table 1.

Transient Absorbance Measurements of Stimulated Emission. The absorbance changes as a function of time were recorded in the wavelength region between 840 and 960 nm for wild type and each of the three mutants. The top panel of Figure 2, which displays the wild type data, shows the decay of the absorbance change at 930 nm as a function of time. The dominant contribution to the absorbance changes at early times in this region in wild type reaction centers is from stimulated emission [Kirmaier & Holten 1988a; for reviews see Kirmaier and Holten (1987) and Woodbury and Allen (1995)]. The wild type absorbance changes between 880 and 970 nm were fitted to two exponential decay terms and a constant:

$$A_0(\lambda) + A_1(\lambda)e^{-t/\tau_1} + A_2(\lambda)e^{-t/\tau_2} \qquad (1)$$

In eq 1, $A_i(\lambda)$ are the amplitude spectra shown in the Figure 2 insets where λ is the wavelength. The time constants, τ_i, are shown associated with the appropriate amplitude spectra in the insets. Fitting the wild type data to only one exponential decay term and a constant resulted in a statistically inferior fit (a 15% increase in the χ^2), and at some wavelengths the fitting residuals clearly deviated from zero beyond the noise limitations of the data. Though in all fits two exponential decay terms and a constant were required, the value of the time constants (τ_i) depended strongly on the time scale of the measurement (data were taken on 15, 50, and 100 ps time scales) and the wavelength region over which the fit was performed. Depending on these factors, the shorter of the two time constants ranged from 1.2 to 1.5 ps, and the longer one ranged from 4 to 14 ps. Apparently the decay of the stimulated emission is not well described by the sum of a small number of exponential decay terms. Complex decay kinetics of P* have previously been observed in *Rb. capsulatus* reaction centers (Du et al., 1992; Chan et al., 1991) as well as in reaction centers of *Rb. sphaeroides*

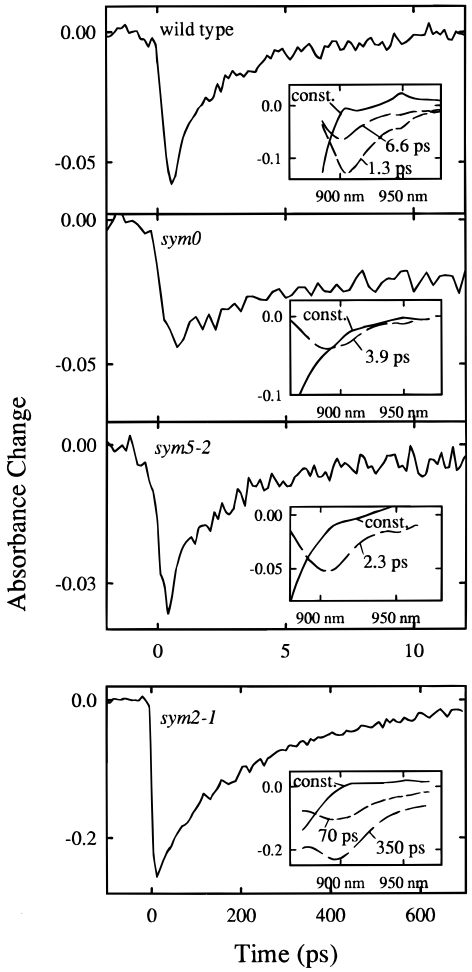

FIGURE 2: The decay of the stimulated emission at 20 K and 930 nm (*Rb. capsulatus* wild type reaction centers), 920 nm (*sym5−2* reaction centers), or 910 nm (*sym0* and *sym2−1* reaction centers). Note that the time scale of the absorbance changes in *sym2−1* reaction centers is roughly 50 times longer than the other samples. Excitation was at 860 nm with a 150 fs pulse. The insets in each panel show the amplitude spectra, $A_i(\lambda)$, and their associated time constants, τ_i, that result from globally fitting the absorbance change kinetics every 2 nm over the indicated wavelength range to either one exponential decay term and a constant (*sym0* and *sym5−2*: $A_0 + A_1(\lambda)\exp(-t/\tau_1)$) or two exponential decay terms and a constant (wild type and *sym2−1*: $A_0 + A_1(\lambda)\exp(-t/\tau_1) + A_2(\lambda)\exp(-t/\tau_2)$).

(Kirmaier and Holten, 1990; Müller et al., 1992; Hamm et al., 1993; Vos et al., 1991; Woodbury et al., 1994). A representative fit is shown in the inset to the wild type panel in Figure 2 which resulted in exponential decay times of 1.3 and 6.6 ps. This was a global fit over 100 transient absorbance spectra taken at 150 fs intervals between 880 and 970 nm. The amplitude spectra of the two rapidly decaying components in wild type reaction centers peak at 906 nm (1.3 ps) and 902 nm (6.6 ps), implying a time-dependent shift of the stimulated emission to higher energy on this time scale. This feature, a time-dependent blue shift of the stimulated emission, was independent of the time scale of the fit. A shift of this nature has been observed previously in mutant reaction centers from *Rb. sphaeroides* at low temperature (Nagarajan et al., 1993).

Figure 2 also shows the decay of the stimulated emission for each of the mutants. In each case, kinetics are shown at a wavelength just to the lower energy side of the stimulated emission peak (920 nm for *sym5−2* and 910 nm for both

sym0 and *sym2−1*). The decay of the stimulated emission from *sym0* on the 20 ps time scale was adequately fit with a single-exponential decay term and a constant to within the signal-to-noise of the data (Figure 2). Due to low yields of reaction centers from the *sym0* mutant, the concentration, and thus the signal-to-noise ratio, for this sample was lower than wild type. The time constant for the stimulated emission decay is 3.9 ps. There is no obvious 1 ps component in this data. Fits of a data set taken over a 100 ps time scale required two exponential decay components with time constants of 2 and 40 ps as well as a constant term for an adequate description of the data (data not shown). On this time scale, the 2 ps component's lifetime is not well resolved, but it has an amplitude roughly three times that of the 40 ps component. The spectral peak of the stimulated emission occurs at higher energy in *sym0* (890 nm) than in wild type (about 905 nm), and in the longer time scale data there is a several nanometer shift of the stimulated emission to higher energy with time (data not shown).

Like wild type, global fitting of the absorbance changes in the stimulated emission region for *sym2−1* reaction centers required at least two exponential decay terms and a constant term for an adequate description (70 and 350 ps with the longer decay term having the dominant amplitude). However, for *sym2−1*, the decay time constants were nearly a factor of 100 longer than those observed in wild type (Figure 2, bottom panel). Using only one exponential decay term and a constant for the global fit resulted in a 15% increase in χ^2 and clearly showed systematic deviations from zero in the fitting residuals. When short time data (15 ps time scale) are globally fit in the 860−970 nm region, a fast component of about 5 ps lifetime is observed, with an amplitude of about 25% of the total decay. On this time scale, there is also a shift of the stimulated emission spectrum by several nanometers toward higher energy with time (data not shown).

Reaction centers from *sym5−2* show a decay of the stimulated emission which is similar to wild type on the 15 ps time scale. Only a single-exponential decay term with a time constant of 2.3 ps was required for the fit, rather than the two exponential decay times used in the wild type, but the signal-to-noise ratio in the *sym5−2* decay trace is somewhat lower than that for wild type, again due to limited sample resulting in small signals. In this case, increasing the number of exponential decay terms only improved the χ^2 by about 5%.

Absorbance Change Spectra as a Function of Time between 730 and 970 nm. Figure 3 shows the time-resolved absorption difference spectra between 730 and 970 nm at various times after excitation. Spectra were taken in two overlapping spectral regions (730−860 nm and 830−970 nm) and were normalized in the overlapping wavelength range near 850 nm. One hundred time-resolved spectra were recorded at different times in each experiment. Three of these spectra are shown in Figure 3 for wild type and each of the mutants.

The 20 K spectra shown for wild type reaction centers follow a time course similar to that seen previously [Kirmaier & Holten, 1988a; for reviews see Kirmaier and Holten (1987) and Woodbury and Allen (1995)]. At 0.4 ps, the prominent spectral features are the presence of the stimulated emission in the 910 nm region, the large bleaching of the Q_Y band of P peaking at about 870 nm, a narrow absorbance increase

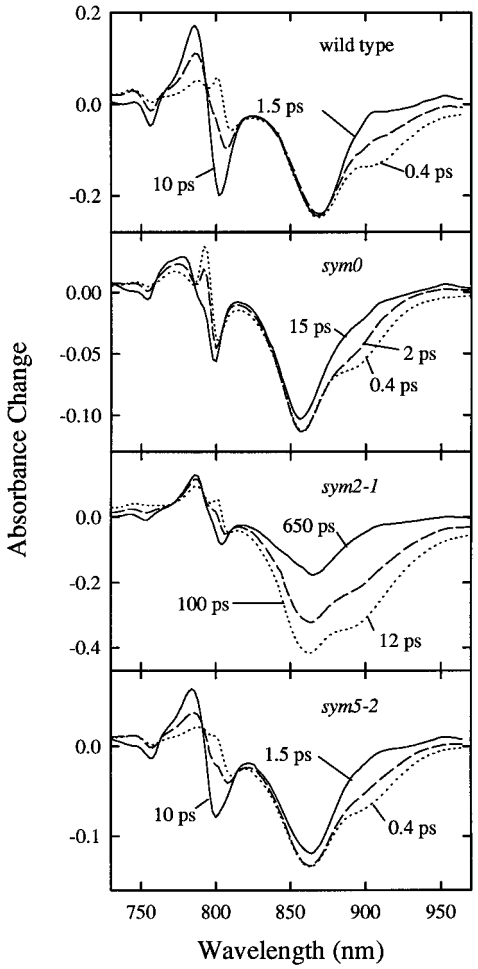

FIGURE 3: Time-resolved transient absorbance spectra at 20 K of reaction centers from wild type *Rb. capsulatus*, *sym0*, *sym2−1*, and *sym5−2*. Times are as indicated. These traces were taken in two wavelength sections, from 730 to 870 nm and from 830 to 970 nm, using a dual diode array spectrophotometer arranged to observe a 140 nm region in 2 nm increments during any single measurement. The spectra in the two regions were merged by normalization and averaging between 830 and 870 nm. Excitation was at 860 nm with a 150 fs pulse. The probe polarization was at the magic angle relative to the excitation pulse polarization.

near 800 nm accompanied by a broader absorbance increase near 790 nm, and a small but significant absorbance decrease near 757 nm. As electron transfer proceeds, further bleaching near 757 nm occurs, presumably due to reduction of H_A, accompanied by a small absorbance decrease near 740 nm (shown in more detail below). The large absorbance increase at 785 nm and decrease at 805 nm in the charge-separated state have been assigned to a shift of one or both of the monomer bacteriochlorophyll transitions to higher energy [see Kirmaier and Holten (1987) for a review]. During the same time period, the stimulated emission in the 910 nm region decays, leaving the Q_Y bleaching of the P band at 870 nm as the dominant feature to the lower energy side of 820 nm in the 10 ps spectrum. These changes occur with three approximate isobestic points at 764 and 794 nm and between approximately 820 and 860 nm. Similar isobestic points have been observed in the low-temperature transient absorbance spectra of *Rb. sphaeroides* (Kirmaier & Holten, 1988b).

The spectral evolution in the *sym0* mutant (Figure 3) is different from that observed in wild type. In the excited state, the absorbance increase near 800 nm is more pro-

nounced, narrower, and shifted to higher energy. It is accompanied by an absorbance decrease on the lower energy side which is also more pronounced than that seen in wild type (relative to the absorbance decrease in the Q_Y band of P). The absorbance decrease near 755 nm during electron transfer in this mutant is not as large as it is in wild type (this may be partly due to incomplete electron transfer after 20 ps in Figure 3, since there is a minor 40 ps component to the charge separation reaction, see above) and the absorbance increase seen in the charge-separated state near 780 nm is broader than that in wild type and less pronounced compared to other spectral features (Figure 3). The peak intensity of the stimulated emission appears to be smaller in *sym0* than in wild type and shifted roughly 15 nm to higher energy. There is little recovery of the ground state bleaching in the 840−850 nm region with time, even on the 100 ps time scale (data not shown), indicating that the overall yield of charge separation in this mutant is high (see below).

The mutant *sym2−1*, which shows the largest changes in the kinetics of electron transfer, has a charge-separated state formed after 650 ps which is spectrally similar to that observed in the wild type, with the exception of some apparent additional bleaching in the 825−850 nm region (Figure 3). However, there are several significant differences in the early time evolution of the system. There is clearly a large recovery of the ground state bleaching in the 840−850 nm region in this mutant, indicating that the yield of electron transfer is low (see Discussion for a quantitative estimate). In addition, the early time spectra show little if any bleaching of the 755 nm band at early times (Figure 4), in contrast to the results in wild type and the other mutants, and the size of the stimulated emission band at 12 ps appears to be enhanced and substantially blue shifted relative to wild type. At 0.4 ps, the stimulated emission band is even slightly more pronounced than at 12 ps (data on the 0.4 ps time scale for *sym2−1* were only taken in the 820−960 nm region and thus a complete spectrum over all of the NIR bands is not shown in Figure 3).

The *sym5−2* mutant (Figure 3) behaves more like the wild type than any of the other mutants considered here. The early time absorbance increase near 800 nm is somewhat less pronounced than in the wild type, and the position of the stimulated emission transition is shifted about 10 nm to higher energy, but the time-dependent spectra are generally analogous to those seen in Figure 3 for wild type reaction centers.

A more detailed picture of the spectral evolution in the 730−770 nm region for wild type and the three mutants is shown in Figure 4. Wild type reaction centers show a substantial bleaching at about 757 nm even at very early times (0.4 ps). This is similar to previous low-temperature results in *Rb. sphaeroides* (Vos et al., 1991; Woodbury et al., 1995). With time, the bleaching in this region increases, presumably reflecting the formation of the bacteriopheophytin anion. In addition to the major absorbance decrease at 757 nm, there is a smaller, broader absorbance decrease observed near 738 nm. Looking at the ground state absorbance spectrum of wild type reaction centers (Figure 1) one can see that the 755 nm transition is asymmetric, with a shoulder on the higher energy side. In fact, the absorbance decrease seen at 757 nm in Figure 4 appears to be narrower than the total ground state absorbance band in Figure 1. This is presumably because the bacteriopheophytin on the A side

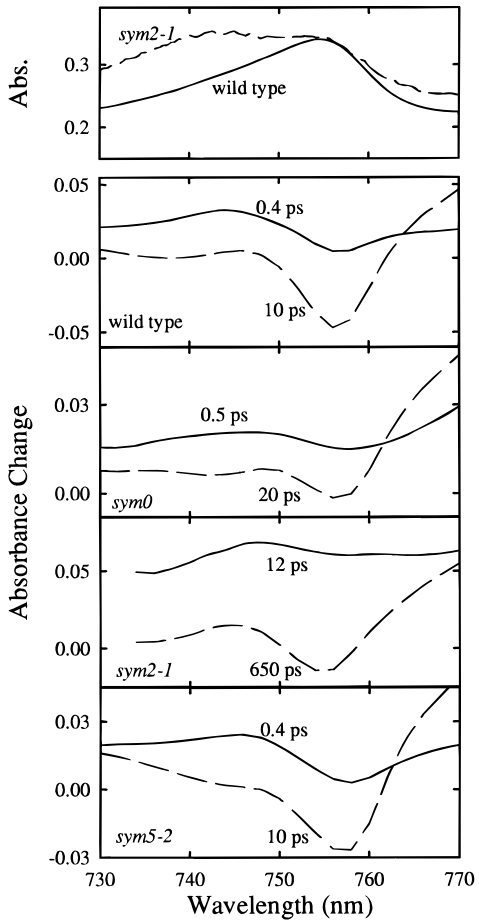

FIGURE 4: Top panel: ground state spectra of *Rb. capsulatus* wild type and *sym2−1* reaction centers between 730 and 770 nm. Lower panels: transient absorbance spectra in the 730−770 nm region of wild type, *sym0*, *sym2−1*, and *sym5−2* reaction centers. The data shown are the same as those in Figures 3 and 4 but are expanded to show this spectral region.

predominantly gives rise to the lower energy part of the 755 nm ground state band, as has been determined for *Rb. sphaeroides* reaction centers based on selective formation of H_A^- and H_B^- via optical pumping techniques (Robert et al., 1985). The broader transition centered near 740 nm in the ground state spectrum which makes the bacteriopheophytin Q_Y transition asymmetric presumably reflects the transition of H_B (Robert et al., 1985) and is in roughly the same position as the broader, weaker absorbance decrease observed in the 10 ps wild type spectrum of Figure 4 at about 738 nm.

In *sym0*, the dip in the early time absorbance spectrum near 755 nm is less pronounced than the analogous 757 nm feature in wild type, and in *sym2−1*, this feature is essentially absent at 0.4 ps, becoming significant only after 20 ps (Figure 4). In all of the mutants, a bleaching of the 755−760 nm ground state absorbance band becomes larger as initial charge separation proceeds. As in wild type, the growth of this feature is accompanied by a dip in the absorbance spectrum between 733 and 743 nm, depending on the sample. The relative size of the 733−743 nm feature varies from mutant to mutant. In the longer time difference absorbance spectra of *sym2−1* (Figure 4, third panel, 650 ps), the extent of the bleaching of the band in this region is more significant than that seen in wild type (Figure 4, first panel, 10 ps), relative to the magnitude of the absorbance decrease in the Q_Y band of P. The 20 K ground state absorbance spectrum in the Q_Y

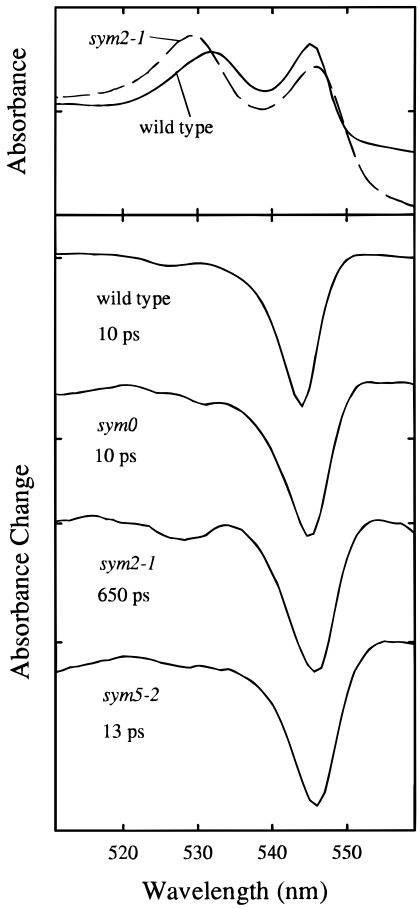

FIGURE 5: Top panel: Ground state spectra of *Rb. capsulatus* reaction centers from wild type and *sym2−1* in the 510 to 560 nm region at 20 K. Expanded from Figure 1. Lower panel: transient absorbance spectra of *Rb. capsulatus* reaction centers from wild type, *sym0*, *sym2−1*, and *sym5−2* at 20 K in the 510−560 nm region excited at 860 nm. Times as indicated. Data was collected simultaneously over the spectral region shown using a dual diode array spectrophotometer. One point is shown every 2 nm.

region of the bacteriopheophytins in *sym2−1* (Figure 1) shows two resolved transitions. The higher energy transition is apparently shifted to the blue relative to the wild type by several nanometers. In the transient absorbance spectra of Figure 4, one can see that there is a greater absorbance decrease between the excited state and $P^+H_A^-$ in the 730−745 nm region of *sym2−1* than in any of the other samples. This could be due in part to additional bleaching of the higher energy bacteriopheophytin transition of *sym2−1*, though there are apparently other absorbance changes in this region as well.

Q_X Transitions of the Bacteriopheophytins. The A and B side bacteriopheophytins can be distinguished spectrally in the Q_X transition region at low temperature [for a review, see Kirmaier and Holten (1987)]. In wild type *Rb. capsulatus*, the maximal ground state absorbance of H_A is at approximately 545 nm at 20 K and that of H_B is at 532 nm (Figures 1 and 5). The spectral resolution of these two bands has made it possible to distinguish between electron transfer resulting in H_A^- formation versus H_B^- formation by observing the bleaching of the ground state spectrum in this region shortly after the initial electron transfer reaction is complete.

Figure 5 shows the absorbance changes that occur upon charge separation in the Q_X transitions of the bacteriopheophytins for wild type and the three *Rb. capsulatus* mutant reaction centers. The absorbance changes observed for wild type in this region are similar to previously published data [reviewed by Kirmaier and Holten (1987) and Woodbury and Allen (1995)]. There is a prominent bleaching of the H_A ground state transition at 545 nm and a very small absorbance change feature near 525 nm. Similar spectral changes are observed in *sym0* and *sym5−2* reaction centers. There is a small, but significant, absorbance decrease at the position of the higher energy absorbance band of the bacteriopheophytin in *sym2−1*.

DISCUSSION

Effects of Symmetry on the Rate and Yield of Electron Transfer. In the preceding article of this issue (Taguchi et al., 1996), it was shown that large-scale symmetry mutations near the cofactors involved in the initial electron transfer reaction and their symmetry related counterparts generally do not result in loss of the ability to grow photosynthetically. The one exception to this rule was *sym0*, but in this case it was possible to isolate genomic suppressor mutations which allowed photosynthetic growth, implying that it was the stability of the photosynthetic unit, rather than the inherent activity of the reaction center, which resulted in the loss of photosynthetic growth capability.

These results are consistent with the measurements of electron transfer rates and yields of charge separation shown in the present report. Each of the isolated reaction centers were capable of charge separation. Note that a detailed discussion of initial electron transfer rates and yields, particularly in some of the mutants, is complicated by the fact that charge separation in both mutant and wild type reaction centers does not occur with single exponential kinetics [see Woodbury and Allen (1995) for a review]. However, it is possible to consider the dominant charge separation kinetics, which presumably dictates the overall ability of the reaction center to function. It is also possible to talk about the yield of photochemistry at a particular time, defined as the amount of the P band in the 840−850 nm region that remains bleached (Woodbury et al., 1994), even though this may not represent the yield of a particular spectrally distinct state.

The *sym0* and *sym5−2* mutants both underwent charge separation with rates (Figure 2) and yields (Figure 3) approaching wild type values, though in the case of *sym0*, there is a minor longer time component associated with charge separation on the tens of picosecond time scale. The discrepancy between the 10 ps value of the P* decay time in *sym0* reaction centers measured by transient absorbance and the roughly 40 ps value reported from time-correlated single-photon counting measurements (Taguchi et al., 1996) comes from the fact that the P* decay in this mutant is not single exponential, and the single photon counting measurements, which are done on the nanosecond time scale, tend to weight the longer components in the fitting. Assuming that at 850 nm the only absorbance change of significance at any time after excitation is ground state bleaching, the yield of electron transfer for wild type, *sym0*, and *sym5−2* can be estimated to be greater than 90% [see Taguchi et al. (1992) or Woodbury et al. (1995) for a detailed discussion of yield estimates]. This is true for *sym0* even after 90 ps when most of the slower (40 ps) component of charge separation is complete (data not shown).

The mutant *sym2−1* gave a much slower overall rate of electron transfer (Figure 2), but even in this mutant, there was a significant yield of the final charge-separated state (Figure 3). Again judging from the recovery of the ground state absorbance at 850 nm, this yield is estimated to be about 35% after 650 ps in quinone-reduced reaction centers at low temperature. Measurements of this mutant at room temperature have indicated that the overall rate of electron transfer is about $(10\ ps)^{-1}$ (data not shown) with yields of $P^+H_A^-$ and $P^+Q_A^-$ formation of 80%−90%. Note that the spectroscopy of this mutant at room temperature is ionic strength dependent, and a complete analysis of ionic strength effects on electron transfer rates has not been performed. At low temperature, the ionic strength effects on the spectrum disappear (to be published elsewhere).

One of the most significant changes in *sym2−1* is the Tyr to Phe change at M208. It has been shown previously that the time constant for electron transfer increases from about 3.5 ps in the wild type to about 10 ps in the Tyr to Phe mutant at 295 K (Nagarajan et al., 1990, 1993; Finkele et al., 1990; Jia et al., 1993) and that the electron transfer rate in this mutant is essentially temperature independent down to about 80 K (Nagarajan et al., 1993; Jia et al., 1993) and then speeds up somewhat at lower temperatures (Jia et al., 1993). However, *sym2−1* undergoes charge separation with a dominant time constant of several hundred ps at 20 K (Figure 2), much longer than the time constant observed for the individual Tyr to Phe mutation. The electron transfer rate and its temperature dependence in the mutant *sym2−1* appear to behave more like the Tyr to Trp mutation at M208 than the Tyr to Phe mutant. The Tyr to Trp mutant (in *Rb. sphaeroides* reaction centers) has a lifetime of about 40 ps at room temperature and about 155 ps at low temperature (Nagarajan et al., 1993). In addition, the P/P^+ midpoint potential of the Tyr to Trp mutant is about 50 meV above wild type (Nagarajan et al., 1993), as it is in *sym2−1* (Taguchi et al., 1996). The *sym2−1* mutation changes six amino acids in a row [see Figure 2 of Taguchi et al. (1996)]. This may have a major effect on the local protein structure which is comparable to introducing a bulky group such as Trp at the M208 position.

Effects of Symmetry on the Ground State and Transient Absorbance Spectroscopy of Reaction Centers. The *sym0, sym2-1,* and *sym5-2* mutations all resulted in a blue shift of both the Q_Y band of P and one of the transitions in the 590 nm region (Figure 1). One can also see in Figure 3 that the stimulated emission band at early times is similarly shifted to higher energy in each of the mutants. This indicates a general destabilization of the P to P* transition in these mutants. Shifting of the Q_Y band of P and increased spectral resolution of transitions in the 590−600 nm region have been seen in a number of mutants in the past [e.g., Taguchi et al. (1992), and Williams et al. (1992)], and may represent a general structural destabilization leading to decreased interaction between the two halves of P.

The mutations *sym0* and *sym2−1* both had significant effects on the ground state reaction center spectra in the 755 and 800 nm regions. As might be expected from the locality of the *sym0* mutation [see Figures 1 and 2 in the preceding article by Taguchi et al. (1996)], one of the monomer bacteriochlorophyll transitions appears to be affected. Comparing to wild type, it appears that the absorbance on the red side of the 802 nm band has decreased, resulting in an apparent shift of the 802 nm band to 800 nm, and a new transition is present in the 790 nm region. This suggests that the long-wavelength side of the 802 nm band in wild type reaction centers is in part due to the B side monomer bacteriochlorophyll, since *sym0* should primarily affect the B side monomer bacteriochlorophyll. This is consistent with the results obtained following reduction of B_B by $NaBH_4$ treatment (Holten et al., 1987; Maroti et al., 1985). There also appears to be a somewhat less pronounced shift to higher energy in *sym0* of a transition within the bacteriopheophytin Q_Y band. The closest bacteriopheophytin to the mutation is H_B. Identification of the lower wavelength bacteriopheophytin as H_B is consistent with previous measurements in *Rb. sphaeroides* (Robert et al., 1985).

As described in the previous paper of this series (Taguchi et al., 1996), it is possible to isolate suppressor mutations which allow *sym0* to grow photosynthetically (the original *sym0* mutant was not photosynthetically viable). Two types of suppressors were found. One has a genomic origin and was used to generate a background strain (*sys0−4*) by curing the original suppressor strain of its plasmid (Taguchi et al., 1996). The *sym0* reaction centers described above were expressed in this background strain. Another type of suppressor showed a single amino acid change within the *sym0* region at M173 and was referred to as *sym0R−4* (Taguchi et al., 1996). This amino acid is normally a proline in *Rb. capsulatus* and is changed to a phenylalanine in the *sym0* mutation. The suppressor mutation involves changing this to a valine, which is the amino acid normally present in the analogous M subunit position of *Rb. sphaeroides* and *Rp. viridis*. The *sym0* region comprises a loop of amino acid sequence including the C−D interhelix region which forms a roof over B_B. At the end of the loop there is a sharp bend which is at least in part defined by the M173 position. Very likely introducing a phenylalanine into this position causes a structural change in the loop which alters the environment of B_B. Consistent with this, the broadening and shifting of the 800 nm band is not observed in the *sym0R−4* suppressor (data not shown). As a final check, the *sym0−R4* suppressor mutation was constructed into a fresh plasmid (ensuring that there were no additional mutations anywhere else in the plasmid) and again an essentially wild type infrared spectrum was obtained (to be published elsewhere). The suppressor strain does show other differences from the wild type in terms of its transient spectroscopy and its ground state spectrum in the Q_X region of bacteriochlorophyll (this band is split as in *sym0*). These topics will be explored in a later publication.

Significant differences are seen between the transient absorbance spectra of wild type and those of *sym0* near 800 nm. This is particularly evident in the early time spectra (Figure 3). In the wild type, the substantial absorbance increase near 800 nm could be interpreted as a loss of intensity borrowing from the monomer bacteriochlorophylls to P upon P* formation [this has been seen in calculations of the *Rp. viridis* spectrum upon removal of P; see Parson and Warshel (1987)]. However, the spectral features of this region in *sym0* look less like the loss of intensity borrowing between the monomer bacteriochlorophylls and P, and more like a shift of one of the two bacteriochlorophyll transitions to higher energy. Such a shift could also be part of the spectral changes in this region in the wild type at early times as well.

The *sym2−1* mutation has more pronounced effects on the bacteriopheophytin Q_Y band than seen in *sym0*. In this case the two bacteriopheophytin transitions are nearly resolved. The new band shape is consistent with the higher energy bacteriopheophytin transition shifting toward the blue. However, this is not what would be expected for a mutation which primarily affects the environment of H_A given the previous assignment of the H_B transition to the higher energy side of the 755 nm band in *Rb. sphaeroides* (Robert et al., 1985). The large effects of the *sym2−1* mutation on the bacteriopheophytin Q_Y transitions are not observed in the single site Tyr to Phe mutant at M210 in *Rb. sphaeroides* (Gray et al., 1990), though a similar splitting is observed when this Tyr is replaced by His, presumably due to hydrogen bond formation (Jones et al., 1994). It is likely that the increased resolution of the bacteriopheophytins is due to *sym2−1* changes at positions other than M208 (which corresponds to M210 in *Rb. sphaeroides*).

The early time transient absorbance changes in the 755 nm region are also unique in *sym2−1* in that there is essentially no indication of bleaching of the ground state Q_Y transitions of the bacteriopheophytins (Figure 4). This is in contrast to wild type and the other mutants which all show such a feature at 0.4 ps [Figure 4; see also Vos et al. (1992)]. In this respect *sym2−1* resembles the triple mutant, LH(L131) + LH(M160) + FH(M195) (Lin et al., 1994), which also showed no early time bleaching in the 755 nm region and, like *sym2−1*, showed an enhanced stimulated emission band (Woodbury et al., 1995). It was suggested that in the triple mutant this was due to a decreased charge-separated character of the system on subpicosecond time scales. Other than the large loss of charge separation yield, the transient absorbance spectra at later times for *sym2−1* are similar to those of wild type.

Effects of Symmetry on the Pathway of Electron Transfer. One of the major motives for generating reaction center mutants with increased symmetry is to study the effect of the protein environment on the path of electron transfer. For this reason, measurements of difference spectra in the regions of the Q_X and Q_Y ground state bacteriopheophytin transitions were performed (Figure 5). In the bacteriopheophytin Q_Y band (Figure 4), there is a greater absorbance decrease on the higher energy side (near 740 nm in the wild type) during charge separation in *sym2−1* compared to the wild type. Since the ground state absorbance in this region is thought to be predominantly due to H_B (Robert et al. 1985; Tiede et al., 1987), one could use the enhanced absorbance changes in this spectral region in *sym2−1* as evidence for bleaching of the ground state transition of H_B due to H_B anion formation. However, this interpretation is complicated by the overlap between the H_A and H_B bands, absorbance features present in this region in the excited state (see the 12 ps spectrum in Figure 4, *sym2−1*) and the possibility of small electrochromic shifts in these transitions upon charge separation.

The Q_X transitions of the bacteriopheophytins are better resolved from each other and presumably more cleanly separated from the bacteriochlorophyll transitions than are the bacteriopheophytin Q_Y transitions [though Shkuropatov and Shuvalov (1993) suggested that bacteriochlorophyll transitions may contribute in this region]. Therefore, this region is usually used for studies of electron transfer pathway. As shown in Figure 5, the dominant absorbance decrease observed in each of the reaction center samples peaks near 545 nm. In each case, there is some bleaching on the higher wavelength side near where H_B absorbs. However, the transient spectra observed in the 530 nm region for wt, *sym0*, and *sym5−2* all show featureless changes in this region which do not correspond very well to the ground state absorbance bands (Figure 5). The *sym2−1* mutant shows a more significant bleaching of the higher energy Q_X bacteriopheophytin band. This bleaching is centered at about 528 nm, which is in reasonable agreement with the slightly blue-shifted H_B ground state transition (peaking at 529 nm, Table 1). If one were to interpret the absorbance decrease at 528 nm as B side electron transfer, then one would conclude that between 10% and 20% of the electron transfer in this mutant proceeds along the B side in *sym2−1*. This is similar to the results recently obtained by Heller et al. (1995) for a double mutant that introduced a ligand near the A side bacteriopheophytin changing it to a bacteriochlorophyll (the so-called β mutant; Kirmaier et al., 1991) and a mutation designed to alter the midpoint potential of the A side monomer bacteriochlorophyll (M203 Gly→Asp; Williams et al., 1992). In this double mutant, the transition normally near 545 nm due to H_A was absent, obviating any small absorbance changes due to reduction of H_B. It was suggested that the perturbation of the B_A environment resulted in an increase in $P^+B_A^-$ energy relative to P^*, slowing down A side electron transfer and thus increasing the yield of B side electron transfer (Heller et al., 1995). One could make a very similar argument in the case of *sym2−1*. This mutation should perturb the environment of the A side cofactors (including B_A), making electron transfer along the A-path less favorable and thus, allowing some B side electron transfer to take place. This suggestion is consistent with the results of Gray et al. (1992) who used photopumping methods to generate a steady state population of bacteriopheophytin anion in a single site mutant of *Rb. sphaeroides*, M210(Y→F) (a submutant of *sym2−1*). They found evidence for some electron transfer along the B-branch in this mutant.

Given the similarity of these results to the more spectrally identifiable results of Heller et al. (1995), it is tempting to suggest that a similar level of B side electron transfer may be occurring in *sym2−1* as was seen in the double mutant described by Heller et al. (1995). However, it is difficult to prove that the transient absorbance changes observed represent H_B anion formation and not small band shifts which overlap with the H_A transition and its vibrational overtones in this region.

Whether or not small fractions of the initial charge separation occur along the B branch in some symmetry mutants, the fact remains that no single region of the D or E helices or the C−D interhelical region encompassed by these mutations [including *sym1* which was studied previously both at room temperature (Taguchi et al., 1992) and at low temperature (H. A. Murchison and N. W. Woodbury, unpublished data)] is solely responsible for the asymmetry of electron transfer in the reaction center, at least if one interprets the Q_X region of the bacteriopheophytin spectrum in the traditional way. Though there are a small number of amino acids in the B and C helices which come in close contact with the cofactors involved in the initial electron transfer reaction that are not included in the symmetry mutants studied (e.g., the glutamic acid at L104), about 80% of amino acids which define the asymmetry of the initial

charge separation event are encoded within the regions modified in this study or previous work (Taguchi et al., 1992). While it is still possible that one of the unmutated amino acids is the predominant factor in determining the direction of electron transfer, it seems much more likely, at this point, that many different, nonsequential amino acids are involved. This conclusion is consistent with the results of Steffen et al. (1994) in which effective dielectric constants for the A and B branches of the reaction center were investigated. Their studies indicated that many different amino acid side chains were important in defining the asymmetric environment of the reaction center cofactors, and thus in determining the direction of electron transfer.

The symmetry mutant studies described in this report also point out a problem with the use of femtosecond transient absorbance as an assay for B side electron transfer. Complete symmetrization of the reaction center would presumably result in 50% electron transfer in each direction. This is the best that could be hoped for by simply making the reaction center more symmetric (as opposed to reversing the asymmetry, a more involved, but potentially interesting approach). Estimates of the ratio of A side vs B side electron transfer in wild type reaction centers vary from study to study, but most suggest that this ratio is large, on the order of 30−100 [e.g., Heller et al. (1995) and Kellogg et al. (1989)]. If multiple amino acids are involved in defining the pertinent asymmetry, then it seems very probable that mutating any single region will change the ratio by less than a factor of 30. If the wild type ratio of A to B side electron transfer is as large as suggested above, then the sensitivity of the transient absorbance measurements performed here might not be high enough to unambiguously detect as much as a factor of 5 change in the ratio. Even when small absorbance changes in the region of H_B ground state transitions are observed (potentially representing 10%−20% B side electron transfer), it is very difficult to distinguish between H_B anion formation and other perturbations of the H_B ground state spectrum, H_A transition vibrational side bands, or changes in underlying absorbing species such as the carotenoid.

ACKNOWLEDGMENT

We thank K. Carty and M. Li for their help with reaction center isolation. The authors also thank Drs. J. Williams, J. Allen, D. Holten, V. Nagarajan, and W. Parson for helpful discussions.

REFERENCES

Allen, J. P., Feher, G., Yeates, T. O., Komiya, H., & Rees, D. C. (1987) *Proc. Natl. Acad. Sci. U.S.A. 84*, 5730−5734.

Breton, J., Martin, J.-L., Migus, A., Antonetti, A., & Orszag, A. (1986) *Proc. Natl. Acad. Sci. U.S.A. 83*, 5121−5125.

Bylina, E. J., Kirmaier, C., McDowell, L., Holten, D., & Youvan, D. C. (1988) *Nature 336*, 182−184.

Chan, C.-K., DiMagno, T. J., Chen, L. X.-Q, Norris, J. R., & Fleming, G. R. (1991) *Proc. Natl. Acad. Sci. U.S.A. 88*, 11202−11206.

Chang, C.-H., El-Kabbani, O., Tiede, D., Norris, J., & Schiffer, M. (1991) *Biochemistry 30*, 5352−5360.

Deisenhofer, J., Epp, O., Miki, K., Huber, R., & Michel, H. (1984) *J. Mol. Biol. 180*, 385−398.

Du, M., Rosenthal, S. J., Xie, X., DiMagno, T. J., Schmidt, M., Hanson, D. K., Schiffer, M., Norris, J. R., & Fleming, G. R. (1992) *Proc. Natl. Acad. Sci. U.S.A. 89*, 8517−8521.

Ermler, U., Fritzsch, G., Buchanan, S. K., & Michel, H. (1994) *Structure 2*, 925−936.

Feher, G., Allen, J. P. Okamura, M. Y., & Rees, D. C. (1989) *Nature 339*, 111−116.

Finkele, U., Lauterwasser, C., Zinth, W., Gray, K. A., & Oesterhelt, D. (1990) *Biochemistry 29*, 8517−8521.

Gallo, D. M, Jr. (1994) Ph.D. Thesis, Arizona State University, Tempe, Arizona.

Gehlen, J. N., Marchi, M., & Chandler, D. (1994) *Science 263*, 499−502.

Gray, K. A., Farchaus, J. W., Wachtveitl, J., Breton, J., & Oesterhelt, D. (1990) *EMBO J. 9*, 2061−2070.

Gray, K. A., Wachtveitl, J., & Oesterhelt, D. (1992) *Eur. J. Biochem. 207*, 723−731.

Hamm, P., Gray, K. A., Oesterhelt, D., Feick, R., Scheer, H., & Zinth, W. (1993) *Biochim. Biophys. Acta 1142*, 99−105.

Heller, B. A., Holten, D., & Kirmaier, C. (1995) *Science 269*, 940−945.

Holten, D., Windsor, M. W., Parson, W. W., & Thornber, J. P. (1978) *Biochim. Biophys. Acta 501*, 112−126.

Holten, D., Kirmaier, C., & Levine, L. (1987) in *Progress in Photosynthetic Research* (Biggins, J., Ed.) Vol. 1, pp 169−175, Martinus Nijhoff, The Hague.

Jia, Y., DiMagno, T. J., Chan, C.-K., Wang, Z., Du, M., Hanson, D. K., Schiffer, M., Norris, J. R., Fleming, G. R., & Popov, M. S. (1993) *J. Phys. Chem. 97*, 13180−13191.

Jones, M. R., Heer-Dawson, M., Mattioli, T. A., Hunter, C. N., & Robert, B. (1994) *FEBS Lett. 339*, 18−24.

Kaufmann, K. J., Petty, K. M., Dutton, P. L., & Rentzepis, P. M. (1976) *Biochem. Biophys. Res. Commun. 70*, 839−845.

Kellogg, E. C., Kolaczkowski, S., Waiselewski, M. R., & Tiede, D. M. (1989) *Photosynth. Res. 22*, 47−59.

Kirmaier, C., & Holten, D. (1987) *Photosynth. Res. 13*, 225−260.

Kirmaier, C., & Holten, D. (1988a) *Israel J. Chem. 28*, 79−85.

Kirmaier, C., & Holten, D. (1988b) *FEBS Lett. 239*, 211−218.

Kirmaier, C., & Holten, D. (1990) *Proc. Natl. Acad. Sci. U.S.A. 87*, 3552−3556.

Kirmaier, C., & Holten, D. (1993) in *The Photosynthetic Reaction Center* (Deisenhofer, J., & Norris, J. R., Eds.) Vol. 2, pp 49−70, Academic Press, San Diego, CA.

Kirmaier, C., Holten, D., & Parson, W. W. (1985) *Biochim. Biophys. Acta 810*, 49−61.

Kirmaier, C., Gaul, D., DeBey, R., Holten, D., & Schenck, C. C. (1991) *Science 251*, 922−927.

Lin, X., Murchison, H. A., Nagarajan, V., Parson, W. W., Allen, J. P., & Williams, J. C. (1994) *Proc. Natl. Acad. Sci. U.S.A. 91*, 10265−10269.

Lockhart, D. J., Kirmaier, C., Holten, D., & Boxer, S. G. (1990) *J. Phys. Chem. 94*, 6987−6995.

Maroti, P., Kirmaier, C., Wraight, C., Holten, D., & Pearlstein, R. M. (1985) *Biochim. Biophys. Acta 810*, 132−139.

Michel-Beyerle, M. E., Plato, M., Deisenhofer, H., Michel, H., Bixon, M., & Jortner, J. (1988) *Biochim. Biophys. Acta 932*, 52−70.

Müller, M. G., Griebenow, K., & Holtzwarth, A. R. (1992) *Chem. Phys. Lett. 199*, 465−469.

Nagarajan, V., Parson, W. W., Gaul, D., & Schenck, C. C. (1990) *Proc. Natl. Acad. Sci. U.S.A. 87*, 7888−7892.

Nagarajan, V., Parson, W. W., Davis, D., & Schenck, C. C. (1993) *Biochemistry 32*, 12324−12336.

Parson, W. W. (1991) in *Chlorophylls* (Scheer, H., Ed.) pp 1153−1180, CRC Press, Boca Raton, FL.

Parson, W. W., & Warshel, A. (1987) *J. Am. Chem. Soc. 109*, 6152−6163.

Parson, W. W., Chu, Z.-T., & Warshel, A. (1990) *Biochim. Biophys. Acta 1017*, 251−272.

Peloquin, J. M., Lin, S., Taguchi, A. K. W., & Woodbury, N. W. (1995) *J. Phys. Chem. 99*, 1349−1356.

Robert, B., Lutz, M., & Tiede, D. M. (1985) *FEBS Lett. 183*, 326−330.

Shkuropatov, A. Y., & Shuvalov, V. A. (1993) *FEBS Lett. 322*, 168−172.

Steffen, M. A., Lao, K., & Boxer, S. G. (1994) *Science 264*, 810−816.

Taguchi, A. K. W., Stocker, J. W., Alden, R. G., Causgrove, T. P., Peloquin, J. M., Boxer, S. G., & Woodbury, N. W. (1992) *Biochemistry 31*, 10345−10355.

Taguchi, A. K. W., Eastman, J. E., Gallo, D. M., Jr., Xiao, W., & Woodbury, N. W. (1996) *Biochemistry 35*, 3175−3186.

Tiede, D. M., Kellogg, E., & Breton, J. (1987) *Biochim. Biophys. Acta 892*, 294−302.

Visscher, K. J., Bergström, H., Sundström, V., Hunter, C. N., & Van Grondelle, R. (1989) *Photosynth. Res. 22*, 211−217.

Vos, M. H., Lambry, J. C., Robles, S. J., Youvan, D. C., Breton, J., & Martin, J.-L. (1991) *Proc. Natl. Acad. Sci. U.S.A. 88*, 8885−8889.

Vos, M. H., Lambry, J. C., Robles, S. J., Youvan, D. C., Breton, J., & Martin, J.-L. (1992) *Proc. Natl. Acad. Sci. U.S.A. 89*, 613−617.

Williams, J. C., Alden, R. G., Murchison, H. A., Peloquin, J. M., Woodbury, N. W., & Allen, J. P. (1992) *Biochemistry 31*, 11029−11037.

Woodbury, N. W., & Allen, J. P. (1995) in *Anoxygenic Photosynthetic Bacteria* (Blankenship, R. E., Madigan, M. T., & Bauer, C. E., Eds.) pp 527−557, Kluwer Academic Publishers, The Netherlands.

Woodbury, N. W., Peloquin, J. M., Alden, R. G., Lin, X., Lin, S., Taguchi, A. K. W., Williams, J. C., & Allen, J. P. (1994) *Biochemistry 33*, 8101−8112.

Woodbury, N. W., Lin, S., Lin, X., Peloquin, J. M., Taguchi, A. K. W., Williams, J. C., & Allen, J. P. (1995) *Chem. Phys. 197*, 405−421.

Youvan, D. C., Ismail, S., & Bylina, E. J. (1985) *Gene 38*, 19−30.

BI952196Z